Plant Science 350 (2025) 112284

Contents lists available at ScienceDirect

Plant Science

journal homepage: www.elsevier.com/locate/plantsci

Prone to loss: Senescence-regulated protein degradation leads to lower protein extractability in aging tomato leaves

Marietheres Kleuter [a], Yafei Yu [b], Francesco Pancaldi [a], Atze Jan van der Goot [b], Luisa M. Trindade [a,*]

[a] Plant Breeding, Wageningen University, Droevendaalsesteeg 1, Wageningen 6708 PB, the Netherlands
[b] Laboratory of Food Process Engineering, Wageningen University, PO Box 17, Wageningen 6700 AA, the Netherlands

ARTICLE INFO

Keywords:
Solanum lycopersicum – tomato
Protein extraction
Protein degradation
Proteases
Senescence

ABSTRACT

The utilization of proteins extracted from tomato (*Solanum lycopersicum*) leaves as cost-effective resources for human consumption or animal feed has gained interest. Thus, increasing protein extractability from tomato leaves became a new breeding target. However, the genetic factors influencing this trait remains poorly understood. In this study, we analyzed changes in leaf protein content, protein composition, and extraction yield across developmental stages, which are vegetative growth, flowering, fruit-forming, and mature fruit. Moreover, tomato gene expression across developmental stages was also studied, to identify genes underlying variability in leaf protein extraction. Protein extraction yield decreased from 0.51 g/g to 0.01 g/g leaf protein from the vegetative to mature stage. However, total protein content inferred with Dumas combustion analysis did not change over the developmental stages tested, while the protein-to-peptide ratio decreased significantly. To further analyze potential causes underlying the decline of protein-to-peptide ratio, the enzymatic activity of proteases – i.e. the enzymes responsible for protein degradation – and the expression of genes encoding these enzymes was studied along plant development. The overall specific activity of proteases did not change significantly throughout plant development. On the contrary, the gene expression of distinct members of the aspartic, cysteine, and subtilase protease families increased. Overall, our findings suggest that extraplastidic protein degradation likely underlies the protein degradation observed during senescence. In the future, the reduction of the activity of extraplastidic proteases through biotechnology could represent an effective strategy to develop tomato varieties with improved protein extraction yields.

1. Introduction

Leaves of different horticulture crops present a novel source of protein for the food and feed industry. Among these crops, tomatoes (*Solanum lycopersicum*) cover a cultivated area of over 4.9 million hectares worldwide (FAOSTAT, 2023), and generate large quantities of side-products. These side-products consist of mostly leaves, stems and roots, accounting for 40 % of the total plant biomass (Taylor and Fraser, 2011). In turn, tomato leaves are a substantial source of protein, by displaying a protein content of 25–30 % based on dry matter (Abo Bakr, 1982; Yu et al. 2023). An effective use of these proteins requires an enhancement of protein extraction techniques and the breeding of varieties with reduced level of protein extraction inhibitors. Previous research showed that protein extraction yields from tomato leaves decreases with plant age, and even more extremely with leaf age (Kleuter et al. 2024; Yu et al. 2023). Specifically, protein extraction yields can drop by a 25-fold factor from young and vegetative to old and senescing leaves along the plant, representing different developmental stages. The biological basis of this drop could partly depend on changes in pectic cell wall components during tomato aging, and partly on other biological factors (Kleuter et al. 2024)

A tomato leaf emerges in response to the need of the plant for photosynthetic products to sustain its growth (Taiz et al. 2015). Since tomato has an indeterminate growth habit, new leaves form mostly at the top of the plant. This results in reduced sunlight exposure of the leaves beneath, leading to a decrease in photosynthetic activity (Heuvelink et al. 2004). This decrease in photosynthetic activity is accompanied by leaf senescence, which happens mostly during the last

* Correspondence to: PO Box 386, Wageningen 6700 AJ, the Netherlands.
E-mail addresses: marietheres.kleuter@wur.nl (M. Kleuter), yafei.yu-woudstra@wur.nl (Y. Yu), francesco.pancaldi@wur.nl (F. Pancaldi), atzejan.vandergoot@wur.nl (A.J. van der Goot), luisa.trindade@wur.nl (L.M. Trindade).

https://doi.org/10.1016/j.plantsci.2024.112284
Received 30 May 2024; Received in revised form 3 September 2024; Accepted 9 October 2024
Available online 15 October 2024

developmental stage of a leaf (Guo and Gan, 2005; Sakuraba, 2021). During leaf senescence, the nutrients in old plant leaves are degraded to provide those to the remaining sink organs, such as young leaves, flowers, or fruits. This degradation involves all macromolecules, such as lipids, polysaccharides, nucleic acids, and also proteins (Buchanan-Wollaston, 1997; Guo and Gan, 2005; Guo et al. 2021; Lim et al. 2007). With regard to proteins, the degradation of chloroplast proteins and the redistribution of the resulting peptides and amino acids is pivotal for the plant (Guo et al. 2021; Kusaba et al. 2009).

The senescence-regulated degradation of proteins from chloroplasts takes place via two distinct pathways: plastidic and extraplastidic (Buet et al. 2019; Otegui, 2018; Zhuang and Jiang, 2019). The plastidic pathway refers to the degradation of proteins within the chloroplasts, where direct protein degradation is carried out by a set of proteases. These proteases are predominantly members of the Clp serine-, Deg serine-, and FtsH metalloprotease families (Adam et al. 2001; Roberts et al. 2012; Van Wijk, 2015). While relevant for plastids biology, the plastidic degradation pathway has a limited impact in senescence-coordinated protein degradation. Contrary, the extraplastidic degradation pathway has a more predominant role, and includes two distinct processes – namely the ubiquitin-proteosome system (UPS) and autophagy (Wang and Schippers, 2019). UPS is a system were single proteins are degraded by first selective ubiquitin tagging and second through degradation within proteasomes (Schreiber and Peter, 2014; Wang and Schippers, 2019). Conversely, autophagy refers to the incorporation of protein complexes and full organelles into the membrane of a phagophore, after which it is trafficked to the vacuole for degradation. As full protein complexes and organelles make up the largest quantity of degradation, autophagy is also often referred to as bulk degradation (Schreiber and Peter, 2014; Wang and Schippers, 2019). Overall, both UPS and autophagy depend on a considerable number of proteases. A large subset of these proteases can be clustered as cystine (Cys) and serine (Ser) proteases (Diaz-Mendoza et al. 2014; Roberts et al. 2012). Notably, most of the proteases, independently of the pathway in which they participate, are encoded by the nuclear genome, thus allowing their identification through transcriptomics data analysis (Guo et al. 2004).

Based on the context just presented, the primary objective of this study was to understand whether protein degradation significantly affects protein extraction yield in tomato leaves across diverse developmental stages. To achieve this objective, various analyses were conducted, including the determination of protein content, protein extraction yield, and protein-to-peptide ratio across leaves from multiple tomato developmental stages (i.e., vegetative, flowering, fruit forming, and mature fruit). Moreover, a specific protease activity assay using two substrates, β-lactoglobulin and RuBisCO to evaluate the enzymatic degradation, and transcriptomics analysis on the same developmental stages were performed, to identify candidate genes that underly differences in protein traits. All the analyses were performed on *Solanum lycopersicum* (tomato) cv. Moneymaker.

2. Material and methods

2.1. Plant material

Seeds of tomato (*Solanum lycopersicum*) cv. Moneymaker from the laboratory of Plant Breeding, Wageningen University, NL, were sown in June 2022 on soil and then transferred first to rockwool blocks and later onto slabs to grow the plant material for this research. The plants were grown under the conditions specified in supplementary Fig. S1 and harvested 119 days after sowing. Every plant was divided into 4 parts, representing the vegetative, flowering, fruit-forming and mature fruit stages (Fig. 1). The vegetative stage was defined as the plant section ranging from the top of the plant until the first flower. The flowering stage contained the leaves between the first flower and the first fruit. The fruit-forming stage contained the leaves between the first fruit and the first red fruit (breaker stage). Finally, all the leaves from the first red fruit until the bottom of the plant were depicted as the mature stage. Three biological replicates corresponding to three individual plants were harvested. From every stage, a subset of leaves was directly shock frozen in liquid nitrogen for the protein analysis using SDS-PAGE, as well as for gene expression analyses, including RNAseq (2.4) and RT-qPCR (2.4.5). The other leaves were taken to the lab for further analyses, namely the assessment of protein content and protein extraction (2.2.1, 2.2.2), high pressure size exclusion chromatography (HPSEC) (2.2.3), and specific protease activity assays (2.3)

2.2. Protein analysis

2.2.1. Protein extraction

Out of the freshly harvested tomato leaves, 5–15 g of material per biological replicate was weighed and blended with 100 mL of MilliQ water (Merck Millipore, Darmstadt, Germany) by an Ultra Turrax (T25

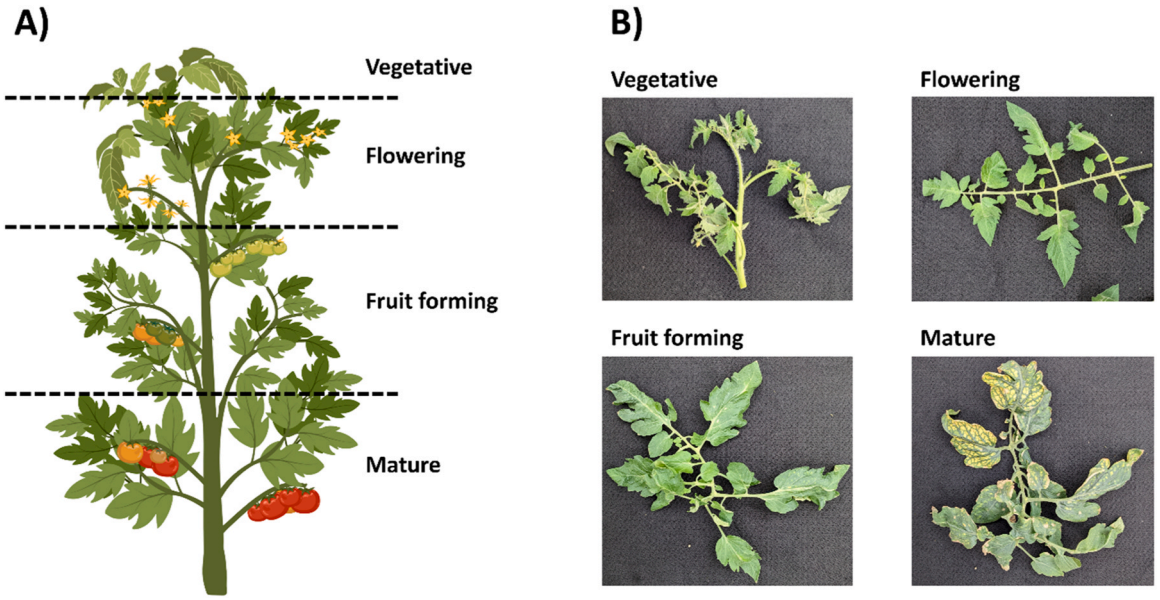

Fig. 1. Scheme of the leaf sampling based on developmental stages (A), and examples of leaves from the corresponding developmental stages (B).

& S 25 N, IKA Labortechnik/Werke GmbH & CoKG, Staufen, Germany) until complete rupture of the leaf ribs. From this suspension, 1.5 mL was taken for the HPSEC analysis and the protease activity assays, following the methodology described in 2.2.3 and 2.3, respectively. The suspension pH was adjusted with 2 M NaOH to pH 11, incubated at 60 °C for 90 min, and subsequently centrifuged (306 g, 5 min, Multifuge 3, Heraeus, Hanau, Germany) to obtain the proteins in the supernatant and leaf fibers in the pellet. After decanting the supernatant, the present proteins were precipitated by adjusting the pH to 4 with 2 M HCl. A second centrifugation step (3928 g, 10 min, Multifuge 3, Heraeus, Hanau, Germany) and decanting of the supernatant resulted in a final protein pellet. This pellet was frozen, freeze dried (< −4 °C, < 3.7 Pa ilShinBioBase Europe, Ede, The Netherlands), weighted, and its protein content was determined with the Dumas analysis as described in 2.2.2.

2.2.2. Assessment of leaf protein content and protein extraction yield

Protein content of the initial tomato leaves was determined on a subset of the harvested leaf material. These tomato leaves were frozen (-20 °C), freeze dried (< −4 °C, < 28mTorr, ilShinBioBase Europe, Ede, The Netherlands), and grinded (A11 basic analytical mill, IKA ®, Staufen, Germany) after harvest. The analysis of leaf protein content and protein content in the pellet was performed with the Dumas nitrogen combustion method using a N exceed analyzer® (Elementar, Langenselbold, Germany). A nitrogen to protein conversion factor of 6.25 was applied (Rhee, 2001) and aspartic acid was used as standard sample. Samples were measured in technical replicates.

Protein yield was determined as the ratio of protein mass in the final extraction pellet and the protein mass in the initial leaves from the harvest, as shown in Eq. 1.

$$Protein\ yield[g \Big/ g leaf\ proteins] = \frac{mass\ of\ extracted\ protein\ in\ final\ pellet[g]}{mass\ of\ protein\ present\ in\ the\ inital\ leaves[g]} \quad (1)$$

2.2.3. Protein composition analysis via High Pressure Size Exclusion Chromatography and SDS-PAGE

To investigate the composition and molecular weight of the leaf proteins, the suspension of blended tomato leaves in MilliQ (from 2.2.1) was centrifuged at maximal speed (13 300 x g) for 15 min and a subset of the supernatant was taken for the analysis. The collected supernatants were fractioned via High Pressure Size Exclusion Chromatography (HPSEC). For this, the Ultimate 3000 HPLC (ThermoFisher, Waltham, USA) with combined columns TSKGel G3000SWXL 5 µm 300 ×7.8 mm and TSKGel G2000SWXL 5 µm 300 ×7.8 mm was used. The temperature of the system was 30 °C and the eluent was 30 vol% Acetonitrile in MilliQ containing 0.1 vol% Trifluoroacetic acid. From each sample, 10 µL was injected at a flow rate of 1.5 mL/min, giving a running time of about 35 min. Detection was based on UV at a wavelength of 214 nm. Quantification was achieved by determination of the area under the curve of the chromatographic peaks. The peaks were categorized into six molecular weight ranges: > 50 kD, 10–50 kD, 4–10 kD, 2–4 kD, 1–2 kD, and 0.5–1 kD. For the separation into these molecular weight ranges, thyroglobulin (670 kDa), phenylalanine (165 kDa), bovine serum albumin (66.5 kDa), β-lactoglobulin (36 kDa), α-lactalbumin (14 kDa), aprotinin (6.51 kDa), and bacitracin (1.42 kDa) were used to create a calibration curve. The relative area of each molecular weight range was taken as a measure of the relative quantity of proteins with a molecular weight within each range. The latter was calculated by dividing the area under the curve corresponding to each range of interest by the total area under the curve. Molecules with a molecular weight >10 kDa were defined as proteins, and molecules with a molecular weight in the range of 10 – 0.5 kDa were defined as peptides. This classification was based on the average protein size of dicot plants. This corresponds to 392 amino acids (Tiessen et al. 2012), equaling a molecular weight of approximately 43 kDa (1 amino acid weights ~110 Da). In parallel, it is known that the smallest 10 % proteins from dicot plants have an average size of about 96 amino acids, corresponding to a molecular weight greater than 10 kDa (Tiessen et al. 2012). In addition, Arabidopsis mini-proteins (< 20 kDa) display a predominant molecular weight of 11 kDa (Kushwaha et al. 2022). By using all these values as references, the relative quantities of proteins (> 10 kDa) and peptides (10 – 0.5 kDa) were determined and from that the protein-to-peptide ratio was calculated according to Eq. 2:

$$Protein - to - peptide\ ratio = \frac{rel.quant\ of\ protein[\%]}{rel.quant\ of\ peptides[\%]} \quad (2)$$

For the protein composition analysis, an SDS polyacrylamide gel electrophoresis (SDS-PAGE) analysis was performed on the shock-frozen leaf material. The analysis was performed with the Bio-Rad Mini-Protein kit (Bio-Rad Laboratories, Hercules, CA, USA) with beta-mercaptoethanol. The shock frozen leaves were grinded (A11 basic analytical mill, IKA ®, Staufen, Germany). About 50 mg of grinded material was placed in an Eppendorf and directly extracted with a mixture of Ripa and 3x Laemmli buffer to receive a protein concentration in the suspension of 10 mg/mL. This mixture was heated up to 95C for 7 min in a heating block and then centrifuged at 13000 rpm at 4C for 15 min. Of the obtained supernatant, 20 µL of sample and 3 or 6 µL of Precision Plus Protein™ All Blue Prestained Protein Standard (Bio-Rad Laboratories, Hercules, CA, USA) were loaded on a 10 % Mini-PROTEAN® TGX™ Stain-free™ gel (Bio-Rad Laboratories, Hercules, CA, USA). The electrophoresis was carried out at 150 V for approximately 1 h. After washing the gel with MilliQ, it was stained with 0.1 % Bio-safe Coomassie Stain (Bio-Rad Laboratories, Hercules, CA, USA) dissolved in methanol, acetic acid and MilliQ (40:10:50). Excessive stain was removed by several washing steps with methanol, acetic acid, and MilliQ (50:10:40). Gels were imaged with the GS-900 Calibrated Densitometer (Bio-Rad Laboratories, Hercules, USA), and the pictures were enhanced in resolution by Image Lab 6.1 (Bio-Rad Laboratories, Hercules, USA).

2.3. Specific proteases activity assay

The protease activity was analyzed based on the protocols of Arbita et al. (2020) and Yu et al. (2024). For this the supernatant of the suspension from blended tomato leaves (2.2.1) after 15 min centrifugation at maximal speed was used. As substrates, β-lactoglobulin (a common standard) and RuBisCO (a representative for plant proteins) were used. Specifically, 500 µL of either 1 % (w/v) β-lactoglobulin or RuBisCO solution in 0.1 M potassium phosphate buffer (pH 7.5) was mixed with 100 µL supernatant. The mixture was then incubated at 37 °C for 10 min. Subsequently, 500 µL of 5 % (w/v) trichloroacetic acid was added to the mixture. The resulting mixture was incubated at 37 °C for 30 min to stop the reaction and centrifuged at 10,000 g for 5 min. An aliquot of 400 µL supernatant was taken and mixed with 1 mL 0.5 M Na_2CO_3 solution and 200 µL 0.5 N Folin-Ciocalteu phenol reagent. The new mixture was incubated at 37 °C for 30 min, followed by centrifugation at 10,000 g for 5 min. Finally, the absorbance of 1 mL supernatant was measured at 660 nm using a DR6000 UV VIS Spectrophotometer (Hach, Colorado, USA). Protease activity was defined in a unit, representing the amount of enzyme hydrolyzing the substrate to produce a color equivalent to 1 µmol (181 µg) of tyrosine per minute. For this, a series of tyrosine solutions (0, 27.5, 55, 110 and 220 µmol/L in 0.1 M potassium phosphate buffer) was used to generate a standard curve. Subsequently the protease activity was calculated with the following equation, taken from Arbita et al. (2020) and Yu et al. (2024):

$$Specific\ protease\ activity[units \Big/ mL\ enyzme] = \frac{TE * vA}{vE * \quad t * vC} \quad (3)$$

In Eq. 3, TE [µmol] indicates the tyrosine equivalent, while vA [mL], vE [mL] and vc [mL] stand for the volume of the total assay, the used enzyme, and the colorimetric measurement (mL), respectively. t [min]

represents the reaction time and cpt [mg proteins/mL supernatant] represents the concentration of proteins in the used supernatant from the blended tomato leaves. The Specific protease activity can further be defined activity per initial dry leaf (Eq. 4) or initial leaf protein (Eq. 5):

$$Specific\ protease\ activity[units/mg\ dry\ leaf] = \frac{SPA}{DL}) \quad (4)$$

$$Specific\ protease\ activity[units \Big/ mg\ initial\ leaf\ protein] = \frac{SPA}{LP} \quad (5)$$

In Eqs. 4 and 5, SPA is the specific protease activity was determined from Eq. 3, while in Eq. 4 DL stands for initial dry leaf [mg/mL] and in Eq. 5 LP stands for initial leaf protein [mg/mL]. Both DL and LP values were received from 2.2.

2.4. Gene expression analysis

2.4.1. RNA sample preparation

Total RNA extraction of ground, shock-frozen tomato leaf samples from the four distinct plant sections and their biological triplicates was performed with the RNeasy Plant Mini Kit (Qiagen, Venlo, The Netherlands) including on-column DNase I digestion. RNA concentrations and purity were measured using the Nanodrop spectrophotometer (Thermo Fischer Scientific, Walkham, MS, USA) and Qubit fluorometer (Qubit 2.0, Invitrogen – Thermo Fischer Scientific, Walkham, MS, USA). RNA quantity was at least above 290 ng/μL and its quality for 260/280 above 2.1 and for 260/320 above 1.95.

2.4.2. Transcriptomic analysis

Transcriptome analysis was performed with RNAseq. From each sample, 2 μg of RNA were diluted in 20 μL MilliQ and sent to BGI (Hongkong) for sequencing. Sequencing was performed on an Illumina HISEQ4000 platform, by first generating Poly-A enriched libraries and then 150 bp paired end reads. An average of 10.13 Gb of data per sample was generated. Raw reads underwent a quality filtering by following the SOAPnuke pipeline (Cock et al. 2010). This included the removal of reads containing adaptors, the removal of reads with N content > 5 % and the removal of low-quality reads. Then, reads were aligned against the *Solanum lycopersicum* genome (ITAG4.0 from Solgenomics Network) by using HISAT2 (Parameters used: –sensitive –no-discordant –no-mixed-I 1 -X 1000 -p 8) (Kim et al. 2015) and Bowtie 2 (Langmead and Salzberg, 2012) for whole genome alignment plus detection of splicing variants, and gene based alignment, respectively.

2.4.3. Identification of differentially-expressed genes

Raw reads were extracted from the provided BGI platform. Differentially-expressed genes were determined by using the DESEQ2 package in R (Version 4.3.0) (Love et al. 2014). Genes with reads of less than 10 were discarded and the samples of the vegetative stage, were set as the reference for analyses. Results were extracted based on the p-adjusted value, determined via Wald-test (alpha < 0.05), multiple-testing correction via Benjamini Hochberg (lfcThreshold = 0, alpha < 0.05), and additional shrinkage of the logarithmic fold change (Zhu et al. 2019). Volcano Plots were generated with the Enhanced-Volcano (2023) package (Blighe et al., 2023).

2.4.4. Identification of tomato proteases

To identify the tomato proteases within the RNA seq data set, a set of 43 functionally validated proteases representing the diversity of these enzymes in plants were collected from the Arabidopsis genome through literature search (Supplementary Table S1). These proteases were annotated for the presence of PFAM motifs by using HMMER3 (default parameters) (Mistry et al. 2013). In parallel, HMMER-based PFAM annotation was also performed for all the tomato genes. For the PFAM analysis, all the PFAM motifs available in Interpro (Paysan-Lafosse et al. 2023) were used. The 43 proteases from Arabidopsis were used as queries in a BLAST ($E = 1E^{-3}$) (Altschul et al. 1990) search against the tomato genome, and the tomato proteases BLAST homologs were further filtered based on PFAM equalities between queries and subjects. In this way, 189 unique tomato proteases were mined from the ITAG4.0 tomato genome.

2.4.5. Gene expression analysis by RT-qPCR

To assess the gene expression of a subset of genes, RNA was freshly extracted from shock frozen tomato leaf samples. The extraction was performed with the RNeasy Plant Mini Kit (Qiagen, Venlo, The Netherlands). After concentration and purity measurement using the Nanodrop spectrophotometer (Thermo Fischer Scientific, Walkham, MS, USA) 1000 ng RNA were taken for DNase I digestion (Qiagen, Venlo, The Netherlands) and subsequent cDNA synthesis with the iScript™ cDNA synthesis kit (Bio-Rad Laboratories, Hercules, USA). Quantitative real-time polymerase chain reaction (RT-qPCR) was performed with IQ™ SYBR Green Supermix (2x) (Bio-Rad Laboratories, Hercules, USA) on a CFX96 Real-Time PCR system (Bio-Rad Laboratories, Hercules, USA). Each reaction volume was in total 10 μL including 5 μL SYBR Green Supermix, 2.5 μL MilliQ, 0.25 μL forward primer, 0.25 μL reverse primer, and 2 μL cDNA template (20 ng). q-PCR amplification cycles encompassed two steps: 1) 95 °C for 15 min, 2) 40 cycles of 95 °C for 15 s, and 60 °C for 1 min. As reference gene the *ELONGATION-FACTOR-1-AlPHA* (EF1a) was used. Primer sequences are provided in Table S4. For each sample technical and biological triplicates were analyzed.

2.5. Statistical analysis

To assess differences in initial protein content, protein extraction yield, HPSEC quantification, specific protease activity, and gene expression quantified by RT-qPCR between experimental samples and developmental plant stages, the data was analyzed statistically by analysis of variance (ANOVA) and post-hoc Tukey test. Differences between the developmental stages were considered as significant when $p < 0.05$. The analysis was performed in R.

3. Results

3.1. Protein extraction yield of tomato leaves decreases with leaf age while protein content remains constant

Proteins were extracted from the leaves corresponding to four developmental stages (vegetative, flowering, fruit-forming, mature fruit) of tomato plants cv. Moneymaker, and protein extraction yield was quantified. This analysis revealed that protein extraction yield from tomato leaves decreased with leaf age. In fact, the yield averaged to 0.51 g/g leaf protein at the vegetative stage, 0.26 g/g at flowering, 0.03 g/g at fruit-forming, and 0.01 g/g at mature fruit stage, respectively (Fig. 2A). These values differ significantly from each other, with the only exception of the protein extraction yield of leaves from the fruit-forming and mature stages. This finding is similar to what was shown in our previous research (Kleuter et al. 2024), where the protein extraction yield was also found to decrease significantly from the top to the bottom sections of tomato plants. Contrary to the protein extraction yields, the protein content remained constant across the four developmental stages, with values ranging between 26.5 % and 29.6 % and no significant differences detected (Fig. 2B).

3.2. Protein-to-peptide ratio is highest in young, vegetative tissue and decreases with aging of the leaves

To investigate the protein profiles of leaves from the different developmental stages of the tomato plants harvested, both SDS-PAGE of shock frozen leaves (Fig. S2) and HPSEC analysis of the leaves blend (Fig. 3) were performed. Results showed that large proteins (>50 kDa), such as the large subunit of RuBisCO were significantly more abundant

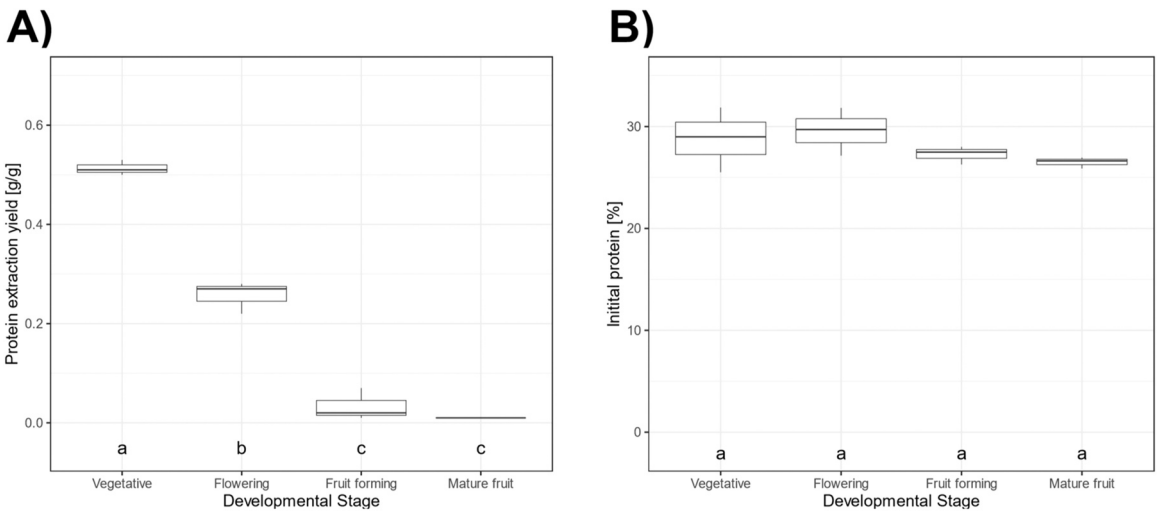

Fig. 2. Protein extraction yield (A) and initial protein content (B) in the tomato leaves from the four different developmental stages assessed in this study: Vegetative, Flowering, Fruit forming, and Mature fruit. The initial protein content was based on Dumas nitrogen combustion analysis with subsequent conversion into protein by a factor of 6.25. Every measurement consists of three biological replicates.

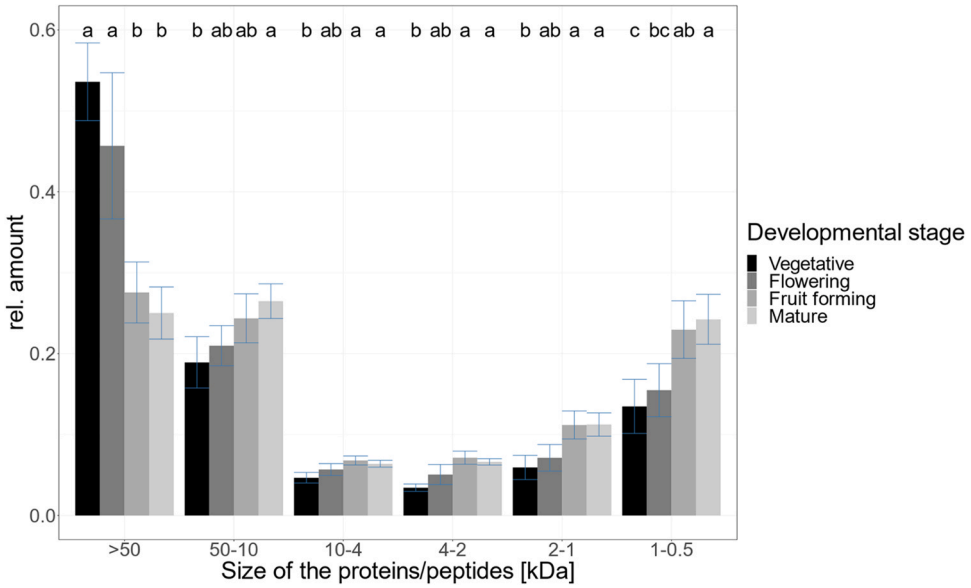

Fig. 3. HPSEC quantification of proteins and peptides across freshly blended material from tomato leaves of vegetative, flowering, fruit forming and mature developmental stages. Every measurement consists of three biological replicates. Letters on the top indicate the significant differences of the relative amount of proteins/peptides between the different developmental stages. Distinct groups of bars along the x-axis correspond to different protein size ranges [kDa].

in leaves from the vegetative and flowering stages than in leaves from fruit-forming and mature stages (Fig. 3). Any smaller proteins (50 – 10 kDa) and peptides (10 – 0.5 kDa) were significantly higher in relative quantity in leaves from fruit-forming and mature stages than in the ones from vegetative and flowering stages (Fig. 3).

The data on the protein and peptide quantities were used to calculate the protein-to-peptide ratios for all developmental stages (proteins: > 10 kDa; peptides: 10 – 0.5 kDa). This ratio was >2 for the vegetative and flowering stages, indicating that twice as many proteins compared to peptides were present (Table 1). Conversely, the fruit-forming and mature stages displayed protein-to-peptide ratios with values close to 1, indicating almost equal amounts of proteins and peptides within the leaves (Table 1). Thus, it can be concluded that leaves from the vegetative and flowering stages store more of their nitrogen in proteins, whereas leaves of later developmental stages have nitrogen stored as both proteins and peptides.

Table 1
Mean protein-to-peptide ratios of leaves at the different developmental stages shown as the average of three biological replicates.

Developmental stage	% Protein out of total N	% Peptide out of total N	Protein-to-peptide ratio
Vegetative	72.5 ± 4.4	27.5 ± 4.4	2.64
Flowering	66.7 ± 5.5	33.3 ± 5.5	2.00
Fruit forming	51.9 ± 5.4	48.1 ± 5.4	1.08
Mature	51.5 ± 4.3	48.5 ± 4.3	1.06

The latter conclusion was further supported by the results of the SDS-PAGE analysis (Fig. S2), which displayed visibly thicker and more intense bands for the material from vegetative and flowering stages than those of the fruit-forming and mature stages, despite equal nitrogen loading. The SDS-PAGEs also display a strong reduction of a ~53 kDa

band, representing the large subunit of RuBisCO (Fig. S2) (Kiskini et al. 2016; Yu et al. 2023). Following these results, the next step entailed the understanding of how the proteases degrade proteins into peptides during plant development, for which a specific protease activity assay was performed.

3.3. Protease activity is constant across developmental stages and higher on the leaf protein RuBisCO

To evaluate the enzymatic activity of proteases across the different developmental stages, a specific protease activity assay with proteases isolated from plant material of the different developmental stages was performed on the dairy protein β-lactoglobulin and on the plant protein RuBisCO (Table 2). In general, the hydrolyzing activity of tomato proteases was higher on RuBisCO than on β-lactoglobulin, independently of the developmental stage. Across the different developmental stages, no significant changes in specific protease activity were identified (Table 2). This was shown for the specific protease activity per supernatant as well as for the activity per dry leaf or initial leaf protein. While the specific protease activity per dry leaf showed a slight maximum at the flowering stage with 0.047 and 0.054 [Units / mg dry leaf] the maximum for the specific protease activity per initial leaf protein at the mature stage was in in the mature stage with 0.248 and 0.284 [Units/mg initial leaf protein] for β-lactoglobulin and RuBisCO, respectively. Following these findings, a transcriptomics analysis was conducted to determine whether specific protease families have a more dominant role on protein degradation at specific developmental stages.

3.4. Proteolytic proteins change in expression from vegetative to mature stage

3.4.1. Several protease genes were differentially expressed along tomato development

To investigate the genetic mechanisms underlying differences in protein extractability from leaves across the four tomato developmental stages, RNAseq analysis was performed on the total RNA extracted from the material collected at each of the four stages. RNAseq data was used to identify differentially-expressed genes between the leaves of the two most extreme stages: vegetative and mature. In total, 22411 genes were identified as expressed genes in the leaves of both stages. Next, the expression dataset was filtered for tomato protease genes, because protease enzymes are responsible for protein degradation (Guo et al. 2021; Wang and Schippers, 2019). As previously mentioned, proteases comprise intra- and extra-plastidic enzymes. To identify all protease genes, a BLAST (Supplementary Table S1) and PFAM-based (Supplementary Table S2) search was conducted with 43 validated proteases from Arabidopsis covering different protease families and subcellular locations. The search identified 189 protease genes in the tomato genome harboring homology with Arabidopsis proteases and proteolytic PFAM domains (Fig. 4). Of these, 77 (40 %) showed differential expression between the vegetative and mature stage (log2fold change > 1 and p-adjusted value < 0.05; red points in Fig. 4; full list in Table S3). Of the 77 differentially-expressed proteases, 56 were downregulated from the vegetative to the mature stage (log_2fold change < -1), while 21 were upregulated (log_2fold > 1). In this study, a focus was set on the upregulated protease genes (Table 3), because an increase in expression likely underlies an increase in their protein degradation activity upon aging (i.e. positive regulation during senescence). The upregulated protease genes where therefore subsequently clustered based on PFAM motif analysis.

Table 2
Specific protease activity (SPA) against β-lactoglobulin and RuBisCO. SPA was quantified in Units/mL using supernatant from blended leaves. Next, the SPA was normalization for the dry leaf content and the initial protein content. The tested proteases originated from blended tomato leaves of four developmental stages: vegetative, flowering, fruit forming, and mature. The data shown represents the mean of three biological replicates including its standard deviation. Small letters behind the values indicate the significant differences between the different developmental stages.

	β-lactoglobulin			RuBisCO		
Sample	SPA [Units/mL]	SPA / dry leaf [Units/mg]	SPA / initial leaf protein [Units/mg]	SPA [Units/mL]	SPA / dry leaf [Units/mg]	SPA / initial leaf protein [Units/mg]
Vegetative	0.579 ± 0.017[a]	0.038 ± 0.006[a]	0.185 ± 0.056[a]	0.683± 0.014[a]	0.045± 0.008[a]	0.219± 0.067[a]
Flowering	0.574 ± 0.007[a]	0.047 ± 0.010[a]	0.237 ± 0.040[a]	0.662± 0.009[a]	0.054± 0.011[a]	0.273± 0.047[a]
Fruit forming	0.582± 0.004[a]	0.031 ± 0.004[a]	0.225 ± 0.046[a]	0.676± 0.012[a]	0.036± 0.005[a]	0.261± 0.055[a]
Mature	0.588 ± 0.018[a]	0.033 ± 0.001[a]	0.248 ± 0.026[a]	0.670± 0.011[a]	0.038± 0.002[a]	0.284± 0.042[a]

3.4.2. Different protease classes display distinct expression patterns throughout tomato development

The 189 tomato protease genes were clustered based on PFAM domains into different protease classes, to determine which protease families play the most dominant roles in leaf senescence and age-regulated protein degradation, based on gene expression data. For the analysis, 22 PFAM configurations corresponding to different protease classes were used (Supplementary Table S2). Of these, three classes showed a significant increase in gene expression when moving from vegetative to mature stages for at least two different genes: cysteine -C1A- proteases (PF00112), aspartic -A1- proteases (PF00026), and serine -S8- proteases (PF00082, also known as subtilases) (Fig. 5). Within these three families, a significant increase in gene expression (log_2fold change > 1 and -log10P < 0.05) was observed for 5 out of 25 cysteine proteases, 5 out of 27 aspartic proteases, and 9 out of 67 subtilases. Upregulation of these genes was found to take place in a progressive and consistent manner across all the developmental stages studied (Fig. 5). Particularly, all aspartic proteases displayed a steady increase throughout the developmental stages, shown by both the RNAseq (Fig. 5 A) and the RT-qPCR results (Fig. S4A, B, C). Furthermore, some cysteine proteases (Solyc02g077040.4, Solyc04g080960.4, Solyc02g076910.3) displayed a slightly higher expression in the fruit forming compared to the mature stage in the RNAseq data (Fig. 5B), while RT-qPCR revealed the peak of Solyc04g080960.4 expression in the mature stage (Fig. S4 D). Regarding subtilase proteases, Solyc02g071560.4, Solyc01g087800.2, Solyc08g079910.2, Solyc08g077860.2 showed a generally steady expression increase across developmental stages based on RNAseq analysis (Fig. 5 C); a pattern observed also in the RT-qPCR results for Solyc02g071560.4 (Fig. S4F). The other five subtilase genes (Solyc08g079860.2, Solyc08g079870.3, Solyc01g087810.2, Solyc01g087820.2, Solyc01g087840.3) displayed a slightly higher upregulation in either the flowering or fruit forming stages compared to the mature stage within the RNAseq data (Fig. 5C). Conversely, Solyc01g087840.3 revealed the lowest expression in the fruit forming stage and the highest in the mature stage, when analyzed by RT-qPCR (Fig. S4E). Overall, these findings suggest that cysteine-, aspartic-, and serine protease genes can likely be considered as leading protease families for protein degradation throughout aging, given the large number of genes from these families showing an increasing expression from the vegetative to the mature stage.

In contrast to cysteine, aspartic, and serine proteases, chloroplast-localized protease genes exhibited negligible expression fluctuations between vegetative and mature tomato developmental stages (Fig. S3). A closer examination of some specific protease families, including Clps, DEGs, and FtsH proteases, revealed even a downregulation for a few

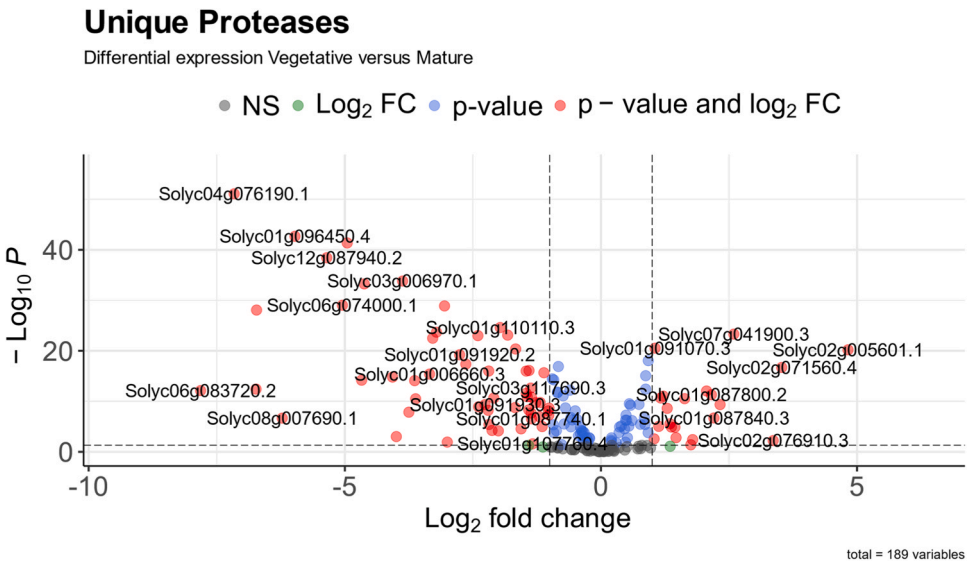

Fig. 4. Volcano plot showing the differential expression of the 189 protease genes identified in the tomato genome. The x-axis displays the $\log_2$ fold change of each protease gene between vegetative and mature stage, while the y-axis depicts the significance ($-\log_{10}$P) of differential changes in gene expression. The analysis was performed on three biological replicates.

Table 3
All 21 upregulated protease genes, showing a log2 fold change (Log2FC) for mature vs. vegetative > 1. The table presents the log2fold Change (Log2FC) and p-adjusted value (padj) for the flowering, fruit-forming, and mature stage versus the vegetative stage, as well as the corresponding protease family and PFAM domains. These genes were received after homology BLAST and PFAM selection.

GeneID	Flowering vs. Vegetative		Fruit forming vs. Vegetative		Mature vs. Vegetative		Protease family	Associated Pfam motifs
	Log2FC	padj	Log2FC	padj	Log2FC	padj		
Solyc02g005601.1	3.659	0.000	4.645	0.000	4.823	0.000	Aspartyl	PF00026; PF14541; PF14543;
Solyc02g071560.4	2.814	0.000	3.429	0.000	3.529	0.000	Subtilase	PF00082; PF05922; PF17766;
Solyc02g076910.3	0.285	0.184	3.822	0.003	3.362	0.006	Cysteine	PF00112; PF03051; PF08246;
Solyc07g041900.3	1.646	0.000	2.402	0.000	2.593	0.000	Cysteine	PF00112; PF03051; PF08246;
Solyc05g016310.1	1.581	0.000	2.483	0.000	2.325	0.000	Aspartyl	PF00026; PF14541; PF14543;
Solyc01g087840.3	2.095	0.000	2.339	0.000	2.206	0.000	Subtilase	PF00082; PF17766;
Solyc01g087800.2	1.814	0.000	2.045	0.000	2.155	0.000	Subtilase	PF00082; PF05922; PF17766;
Solyc01g087810.2	1.905	0.000	2.130	0.000	2.063	0.000	Subtilase	PF00082; PF05922; PF17766;
Solyc08g079910.2	0.351	0.311	1.565	0.011	1.791	0.004	Subtilase	PF00082; PF02225; PF05922; PF17766;
Solyc08g077860.4	0.080	0.740	1.236	0.098	1.756	0.042	Subtilase	PF00082; PF05922; PF17766;
Solyc11g011440.1	0.771	0.002	1.478	0.000	1.634	0.000	Aspartyl	PF00026; PF14541; PF14543;
Solyc08g078550.1	0.496	0.187	1.881	0.000	1.467	0.002	Metallo (M10)	PF00413; PF01471;
Solyc01g087820.2	1.557	0.000	1.404	0.000	1.444	0.000	Subtilase	PF00082; PF05922; PF17766;
Solyc08g079870.3	1.567	0.000	1.752	0.000	1.375	0.000	Subtilase	PF00082; PF02225; PF05922; PF17766;
Solyc08g079860.2	1.341	0.000	1.628	0.000	1.348	0.000	Subtilase	PF00082; PF02225; PF05922; PF17766;
Solyc02g065050.1	0.726	0.001	1.189	0.000	1.295	0.000	Aspartyl	PF00026; PF14541; PF14543;
Solyc04g080960.4	1.022	0.000	1.385	0.000	1.217	0.000	Cysteine	PF00112; PF08246;
Solyc02g069100.4	0.567	0.002	1.098	0.000	1.168	0.000	Cysteine	PF00112; PF08127;
Solyc08g068870.3	0.871	0.001	1.189	0.000	1.129	0.000	Aspartyl	PF00026; PF14541; PF14543;
Solyc01g091070.3	0.286	0.023	0.786	0.000	1.057	0.000	Metallo (M26)	PF00557; PF15801;
Solyc02g077040.4	0.882	0.010	1.231	0.000	1.038	0.003	Cysteine	PF00112; PF03051; PF08246;

members of these families, while upregulation was not observed for any proteases of these classes. This suggests that the overall proteolytic capacity within chloroplasts is maintained or even slightly reduced during leaf senescence.

4. Discussion

This study aimed to provide a long-term perspective on valorizing residual tomato leaves as a potential source of proteins for various applications. To achieve this objective, it was tested if and how (from a genetic point of view) protein degradation during plant development affects potential protein extraction yield from tomato leaves. Recently, the role of plant cell wall, particularly the pectin network, was investigated as a putative limiting factor for protein extraction yields from tomato leaves (Kleuter et al. 2024). While pectins can limit protein extraction yields, other factors are very likely involved in determining the decline in protein extraction yield observed from young to old tomato leaves, too (Kleuter et al. 2024). Here, protein degradation during plant development was therefore studied as a possible alternative driver for such decline of protein extraction yields in aging tomato leaves. Moreover, a secondary goal was the identification of putative genetic targets for enhancing protein extraction yield. Overall, the results showed that a marked degradation of leaf proteins is taking place during plant ageing, which is likely a cause for decreased protein extraction yield attainable from young to old tomato leaves. Moreover, patterns of gene expression displayed by specific classes of proteases make these enzymes and the genes encoding them interesting candidates to explain the observed patterns of protein degradation and decreased protein extraction yields in senescing tomato leaves. In this section, the implications of all these findings are discussed, encompassing both fundamental and applied perspectives.

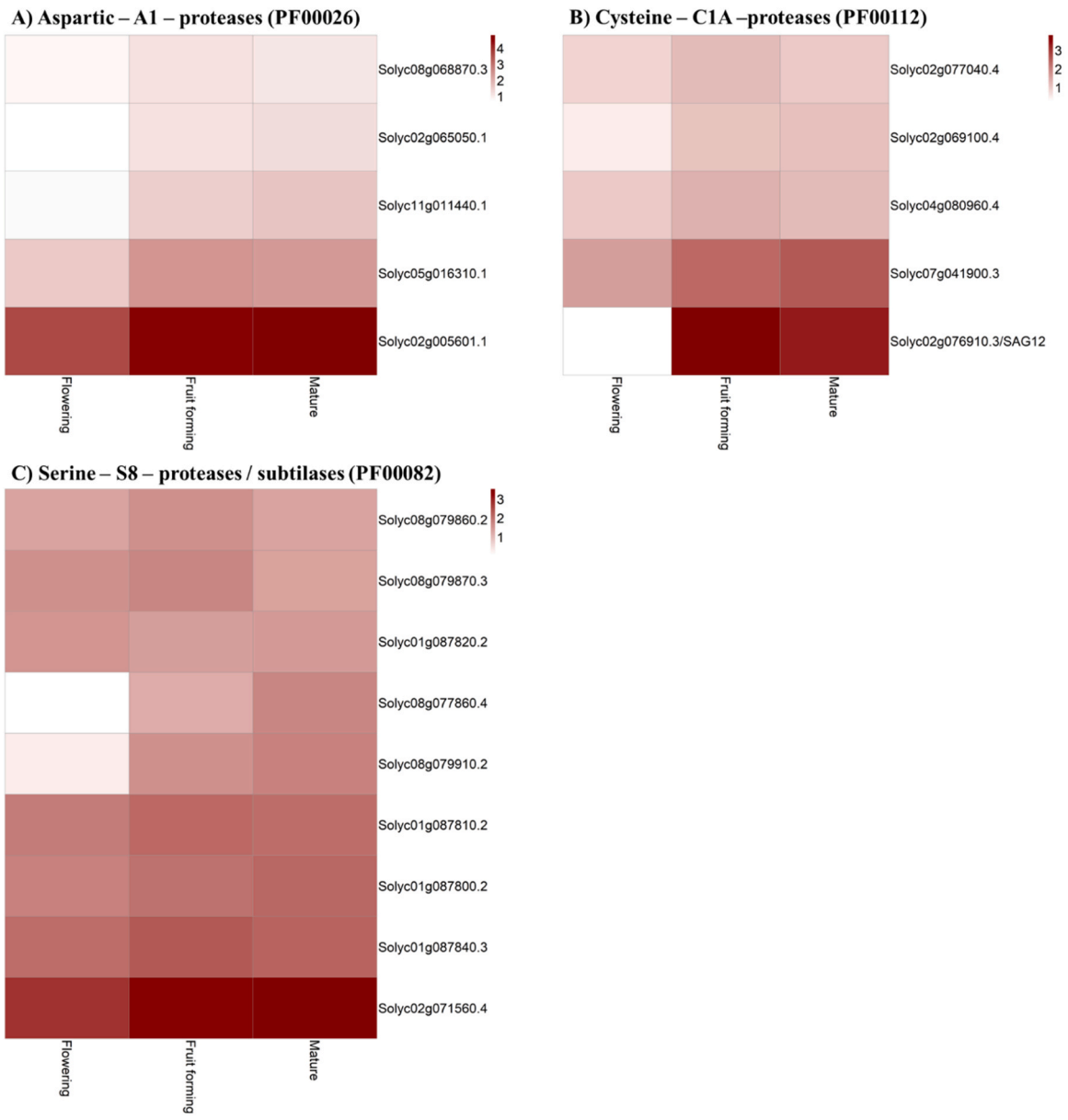

Fig. 5. Representation of protease gene expression analysis using heatmaps. The three panels represent the upregulated proteases of three protease families: aspartic proteases (A), cysteine proteases (B), and serine proteases (C). Columns represent the log2 fold changes between the stages of flowering (Flowering), fruit forming (Fruit forming), and mature fruit (Mature) compared to the vegetative. The log2 fold change is represented by the color gradient from white to red. The rows are labeled with the GeneIDs and if know the protein name.

4.1. Leaf senescence limits protein extraction yield as a result of a decreased protein-to-peptide ratio

A pronounced decrease in protein extraction yield as tomato leaves transition from the vegetative to the mature stage was observed (Fig. 2A). Remarkably, this decrease is not accompanied by a decrease in total nitrogen, as revealed by the total leaf protein content determined by Dumas combustion analysis (Fig. 2B). The results of the HPSEC (Fig. 3) and SDS-PAGE (Fig. S2) analyses provide insights in the reduced amount of protein bound nitrogen, while the amount of peptide bound nitrogen increased along the developmental stages. This result is in line with what was reported by Kiskini et al. (2016), who found that the nitrogen to protein conversion factor needs to be lowered in sugar beet leaves of increasing age. The lowering of the nitrogen to protein conversion factor implies a reduction of protein bound nitrogen throughout leaf ageing, highly likely linked to a decline in RuBisCO content (Kiskini et al. 2016). A reduction of protein bound nitrogen is attributed to protein degradation. In aging tomato leaves, such protein degradation affects the maximal protein extraction yield negatively, due to the fact that smaller proteins and peptides do not precipitate under acidic conditions, as conducted in the last step of the here used protein extraction procedure. Therefore, understanding why and how protein degradation along developmental stages takes place in tomato leaves is of key importance to design strategies to downregulate this process and maximize protein extraction yields.

In a biological context, protein degradation upon leaf senescence is a natural process. During the vegetative and flowering stages, leaves require a diverse array of functional proteins, predominantly those related to photosynthesis, to support the ongoing growth and development of the plant (Omidbakhshfard et al. 2021; Tcherkez et al. 2020). This is underlined by a high protein-to-peptide ratio in vegetative and flowering plant developmental stages, as observed in our study (3.2 and Table 1). With the transition to the fruit-forming stage, a gradual decline in photosynthesis rate occurs, partially attributed to a reduced light

intensity (Heuvelink et al. 2004). Thereafter, degradation of larger proteins, such as RuBisCo, becomes noticeable in lower leaves (fruit forming and mature stage), as detected by HPSEC (Fig. 3) and SDS-PAGE (Fig. S2) analyses. It is known that plants re-allocate nutrients, including peptides and amino acids, to support growth organs, such as leaves of the vegetative and flowering stages, as well as reproduction organs, notably fruits (Buchanan-Wollaston, 1997; Lim et al. 2007). However, in this study no significant reduction in nitrogen content was observed in the leaves of the mature stage (Fig. 2 B). Additionally, the leaves of the mature section were predominantly green (Fig. 1 B). Together these observations suggest that the leaves of the mature stage were at the onset of senescence, where protein degradation occurred but nutrient reallocation was not yet initiated (Gepstein et al. 2003; Hortensteiner and Krautler, 2011; Tamary et al. 2019). As a result, a delay of senescence onset can enhance protein extraction yields from tomato leaves.

4.2. *Senescence-steered leaf protein degradation occurs mainly via extraplastidic pathways*

The reallocation of nutrients, particularly nitrogen, during plant maturation, is a critical process for the plant survival and reproductive success (Guo et al. 2021; Kusaba et al. 2009). As stated above, this process entails also the degradation of proteins as a critical part of nutrient reallocation, primarily performed by various protease genes (Feller and Fischer, 1994; Guo et al. 2004; Guo et al. 2021; Hörtensteiner and Feller, 2002; Lim et al. 2007). Given the negative impact of protein degradation on protein extraction yield from tomato leaves, as identified in this study, the specific enzymatic activity, and the expression rates of several tomato proteases across four developmental stages were examined. Overall, these analyses identified protease genes potentially impacting protein degradation upon leaf senescence.

The enzymatic activity assays revealed that tomato proteases display higher specificity for plant proteins as RuBisCO than dairy proteins such as β-lactoglobulin. Moreover, this activity does not significantly increase or decrease across the developmental stages. Slightly higher specific protease activities were detected when normalized per dry leaf and per initial leaf protein at the flowering and mature stage, respectively. The first observation aligns with the study of van Loon et al. (1987) who reported that protease activities in leaves of oat and tobacco reach their maximum when the leaves are fully expanded, while the second aligns with further findings of this study, stating that protein degradation increases throughout development. However, it is important to note that any *ex-planta* analysis provides information on the activity potential and may not fully translate into *in-vivo* conditions. Therefore, detailed insights can be only obtained through expression analysis.

The expression analysis revealed that the majority of proteases did not show any significant change in their quantity upon maturation (Fig. 4). This was especially the case for most chloroplast-localized proteases, referring to the families of Clps, Degs, and FtsHs. Instances of significant changes in gene expression for these protease families were predominantly characterized by downregulation, stating reduced presence of these proteases in mature leaves (Fig. S3). This suggests minimal impact of plastidic protein degradation throughout development, aligning with the findings of Guo et al. (2004), who did not detect changes in plastidic proteases of Arabidopsis as major upregulated genes during senescence. This was also underlined by a study of Zhang et al. (2007), who showed that RuBisCO degradation is incomplete, when chloroplasts were isolated. A compiled assessment of several senescence association studies from various crops concluded that most chloroplast-localized proteases are involved in protein turnover, cutting of localization signals, or degradation of misfolded proteins (Roberts et al. 2012). These processes are essential for maintaining cellular function and integrity but are thus not relevant to identify target genes driving senescence associated protein degradation.

Contrary to the limited impact of plastidic protein degradation, our study revealed an upregulation of aspartic (A1), cysteine (C1A), and serine (S8) proteases (Fig. 5), which are all classes primarily associated with extraplastidic protein degradation pathways (Beers et al. 2004; Carrion et al. 2013; Feller and Fischer, 1994; Otegui et al. 2005). Most of the upregulated proteases exhibited a progressive increase in gene expression from the vegetative to the mature developmental stage (Fig. 5), correlating with the gradual decrease in protein extraction yield (Fig. 2A). This observation suggests extraplastidic protein degradation as the main degradation pathway associated with leaf senescence. In turn, this suggestion is supported by several compiled studies, in which senescence induced bulk degradation was stated to be strongly driven by autophagy and its associated degradation pathways, including Rubisco-containing bodies (RCBs) and senescence-associated vacuoles (SAVs) (Guo et al. 2021; Ishida et al. 2014; Ishida et al. 2008; Van Wijk, 2015). Notably, it has been demonstrated that proteins internalized in senescence-associated vacuoles, including RuBisCO, undergo complete degradation upon isolation (Martinez et al. 2008), underpinning the importance of this pathway. When referring to the proteases involved in the extraplastidic pathway, our results revealed a strong upregulation of cysteine (C1A) proteases (Fig. 5B). This finding underscores previous research, where cysteine (C1A) proteases have been identified as the most abundant and most upregulated proteolytic enzymes during leaf senescence (Diaz-Mendoza et al. 2014; Guo et al. 2004). Moreover, cysteine (C1A) proteases have been designated as senescence-associated genes (SAGs), with SAG12 being a well-known senescence marker localized within senescence-associated vacuoles (SAVs) (Carrion et al. 2013; James et al. 2018; Lohman et al. 1994; Martinez et al. 2008; Otegui et al. 2005). In our study, we observed a pronounced upregulation of SAG12 (Solyc02g076910.3) (Fig. 5B), underlining the involvement of senescence associated vacuoles in senescence steered protein degradation. Apart from cysteine (C1A) proteases, aspartic (A1) proteases were also shown to be upregulated in leaf senescence (Fig. 5A). This result is noteworthy, since the specific involvement of aspartic (A1) proteases in protein degradation is not well clarified in literature (Gepstein et al. 2003; Roberts et al. 2012). In addition to aspartic and cysteine proteases, serine (S8) proteases, known as the subtilase family, demonstrated an upregulated trend during leaf senescence (Fig. 5 C). This observation aligns with previous studies, where serine (S8) proteases were upregulated upon senescence in Arabidopsis (Martinez et al. 2015) as well as in wheat (Roberts et al. 2012; Roberts et al. 2011). Particularly in wheat, serine (S8) proteases were connected to RuBisCO degradation, suggesting a pivotal role in nitrogen remobilization (Roberts et al. 2011). While limited information is available about the localization of both, aspartic (A1) and serine (S8) proteases, bioinformatics analysis predicted for most members of these families a secretory signal. Interestingly these secretory signals guide the proteases neither to the chloroplasts nor to the mitochondria, but rather suggests their localization within other cytosolic compartments or the extracellular space (Beers et al. 2004), underlining their involvement in protein degradation outside the plastids. Overall, all these considerations, together with our results, support the hypothesis that protein degradation in senescing tomato leaves occurs predominantly via extraplastidic degradation pathways, governed by members of the aspartic (A1), cysteine (C1A) and serine (S8) proteases families.

5. Conclusion

To conclude, our study revealed a reduction in protein extraction yield from young to old leaves, which was primarily attributed to protein degradation. The transcriptomics analysis identified distinct upregulated protease families, predominantly linked to extraplastidic protein degradation pathways. Thus, we hypothesize that this upregulation of distinct protease families underlies the increased protein degradation throughout tomato developmental stages. As a final outcome of these results, future breeding targets to develop varieties with improved protein extractability from leaves should aim at lowering the expression of cysteine, aspartic, and serine proteases participating in the

extraplastidic protein degradation pathway. Specific targeting of these genes can potentially limit the amount of protein degradation, especially in older leaves. This enhances the potential to utilize proteins from agricultural waste.

Funding

This work was supported by Wageningen University Investment team 'Protein Transition'.

Disclosure statement

During the preparation of this work the author(s) used ChatGPT from OpenAI in order to generate a first draft out of bullet points. After using this tool/service, the author(s) reviewed and edited the content as needed and take(s) full responsibility for the content of the publication.

CRediT authorship contribution statement

Luisa M Trindade: Writing – review & editing, Supervision, Project administration, Conceptualization. **Atze Jan van der Goot:** Writing – review & editing, Supervision. **Francesco Pancaldi:** Writing – review & editing, Methodology, Data curation. **Yafei Yu:** Writing – review & editing, Formal analysis. **Marietheres Kleuter:** Writing – original draft, Visualization, Methodology, Formal analysis, Data curation, Conceptualization.

Declaration of Competing Interest

The authors declare that they have no known competing financial interests or personal relationships that could have appeared to influence the work reported in this paper.

Acknowledgements

The authors would like to thank Annemarie Dechesne for her help in the biochemical lab, Fien Meijer-Dekens, and Maarten Peters for their support during the tomato growth in the greenhouse, Maurice Streubl for his support on the HPSEC and Wouter de Groot for his help with the Dumas analyzer.

Appendix A. Supporting information

Supplementary data associated with this article can be found in the online version at doi:10.1016/j.plantsci.2024.112284.

Data Availability

Data will be made available on request.

References

T. Abo Bakr, Leaf protein isolates from some Egyptian crops, Food Chem. 9 (4) (1982) 295–301, https://doi.org/10.1016/0308-8146(82)90081-4.

Z. Adam, I. Adamska, K. Nakabayashi, O. Ostersetzer, K. Haussuhl, A. Manuell, B. Zheng, O. Vallon, S.R. Rodermel, K. Shinozaki, A.K. Clarke, Chloroplast and mitochondrial proteases in Arabidopsis. A Proposed Nomenclature1, Plant Physiol. 125 (4) (2001) 1912–1918, https://doi.org/10.1104/pp.125.4.1912.

S.F. Altschul, W. Gish, W. Miller, E.W. Myers, D.J. Lipman, Basic local alignment search tool, J. Mol. Biol. 215 (3) (1990) 403–410, https://doi.org/10.1016/S0022-2836(05)80360-2.

A.A. Arbita, N.A. Paul, J. Cox, J. Zhao, Extraction, partial purification and characterization of proteases from the red seaweed Gracilaria edulis with similar cleavage sites on kappa-casein as calf rennet, Food Chem. 330 (2020) 127324, https://doi.org/10.1016/j.foodchem.2020.127324.

E.P. Beers, A.M. Jones, A.W. Dickerman, The S8 serine, C1A cysteine and A1 aspartic protease families in Arabidopsis, Phytochemistry 65 (1) (2004) 43–58, https://doi.org/10.1016/j.phytochem.2003.09.005.

Blighe, K., Rana, S., Lewis, M., 2023. EnhancedVolcano: publication-ready volcano plots with enhanced colouring and labeling. https://bioconductor.org/packages/devel/bioc/vignettes/EnhancedVolcano/inst/doc/EnhancedVolcano.html.

V. Buchanan-Wollaston, The molecular biology of leaf senescence, J. Exp. Bot. 48 (1997).

A. Buet, M.L. Costa, D.E. Martinez, J.J. Guiamet, Chloroplast protein degradation in senescing leaves: proteases and lytic compartments, Front. Plant Sci. 10 (2019) 747, https://doi.org/10.3389/fpls.2019.00747.

C.A. Carrion, M.L. Costa, D.E. Martinez, C. Mohr, K. Humbeck, J.J. Guiamet, In vivo inhibition of cysteine proteases provides evidence for the involvement of 'senescence-associated vacuoles' in chloroplast protein degradation during dark-induced senescence of tobacco leaves, J. Exp. Bot. 64 (16) (2013) 4967–4980, https://doi.org/10.1093/jxb/ert285.

P.J. Cock, C.J. Fields, N. Goto, M.L. Heuer, P.M. Rice, The Sanger FASTQ file format for sequences with quality scores, and the Solexa/Illumina FASTQ variants, Nucleic Acids Res. 38 (6) (2010) 1767–1771, https://doi.org/10.1093/nar/gkp1137.

M. Diaz-Mendoza, B. Velasco-Arroyo, P. Gonzalez-Melendi, M. Martinez, I. Diaz, C1A cysteine protease-cystatin interactions in leaf senescence, J. Exp. Bot. 65 (14) (2014) 3825–3833, https://doi.org/10.1093/jxb/eru043.

FAOSTAT, Crop and livestock products. Food and Agriculture Organization of the United Nations., 2023, 2023. ⟨http://www.fao.org/faostat/en/#data⟩.

U. Feller, A. Fischer, Nitrogen metabolism in Senescing leaves, Crit. Rev. Plant Sci. 13 (3) (1994) 241–273, https://doi.org/10.1080/07352689409701916.

S. Gepstein, G. Sabehi, M.J. Carp, T. Hajouj, M.F. Nesher, I. Yariv, C. Dor, M. Bassani, Large-scale identification of leaf senescence-associated genes, Plant J. 36 (5) (2003) 629–642, https://doi.org/10.1046/j.1365-313x.2003.01908.x.

Y. Guo, Z. Cai, S. Gan, Transcriptome of Arabidopsis leaf senescence, Plant, Cell Environ. 27 (5) (2004) 521–549, https://doi.org/10.1111/j.1365-3040.2003.01158.x.

Y. Guo, S. Gan, Leaf senescence: signals, execution, and regulation, Curr. Top. Dev. Biol. 71 (2005) 83–112, https://doi.org/10.1016/S0070-2153(05)71003-6.

Y. Guo, G. Ren, K. Zhang, Z. Li, Y. Miao, H. Guo, Leaf senescence: progression, regulation, and application, Mol. Hortic. 1 (1) (2021), https://doi.org/10.1186/s43897-021-00006-9.

Heuvelink E., Bakker M., Elings A., Kaarsemaker R., Marcelis L. Effect of lEaf Area on Tomato Yield. In: International Conference on Sustainable Greenhouse Systems-Greensys2004 691, 2004. pp 43-50.

S. Hortensteiner, B. Krautler, Chlorophyll breakdown in higher plants, Biochim. Et. Biophys. Acta 1807 (8) (2011) 977–988, https://doi.org/10.1016/j.bbabio.2010.12.007.

S. Hörtensteiner, U. Feller, Nitrogen metabolism and remobilization during senescence, J. Exp. Bot. 53 (370) (2002) 927–937.

H. Ishida, M. Izumi, S. Wada, A. Makino, Roles of autophagy in chloroplast recycling, Biochim. Et. Biophys. Acta 1837 (4) (2014) 512–521, https://doi.org/10.1016/j.bbabio.2013.11.009.

H. Ishida, K. Yoshimoto, M. Izumi, D. Reisen, Y. Yano, A. Makino, Y. Ohsumi, M. R. Hanson, T. Mae, Mobilization of rubisco and stroma-localized fluorescent proteins of chloroplasts to the vacuole by an ATG gene-dependent autophagic process, Plant Physiol. 148 (1) (2008) 142–155, https://doi.org/10.1104/pp.108.122770.

M. James, M. Poret, C. Masclaux-Daubresse, A. Marmagne, L. Coquet, T. Jouenne, P. Chan, J. Trouverie, P. Etienne, SAG12, a major cysteine protease involved in nitrogen allocation during Senescence for seed production in Arabidopsis thaliana, Plant Cell Physiol. 59 (10) (2018) 2052–2063, https://doi.org/10.1093/pcp/pcy125.

D. Kim, B. Langmead, S.L. Salzberg, HISAT: a fast spliced aligner with low memory requirements, Nat. Methods 12 (4) (2015) 357–360, https://doi.org/10.1038/nmeth.3317.

A. Kiskini, A. Vissers, J.-P. Vincken, H. Gruppen, P.A. Wierenga, Effect of plant age on the quantity and quality of proteins extracted from sugar beet (Beta vulgaris L.) leaves, J. Agric. Food Chem. 64 (44) (2016) 8305–8314, https://doi.org/10.1021/acs.jafc.6b03095.

M. Kleuter, Y. Yu, F. Pancaldi, M. Nagtzaam, A.J. van der Goot, L.M. Trindade, Cell wall as a barrier for protein extraction from tomato leaves: a biochemical study, Plant Physiol. Biochem. 208 (2024), https://doi.org/10.1016/j.plaphy.2024.108495.

M. Kusaba, T. Maoka, R. Morita, S. Takaichi, A novel carotenoid derivative, lutein 3-acetate, accumulates in senescent leaves of rice, Plant Cell Physiol. 50 (8) (2009) 1573–1577, https://doi.org/10.1093/pcp/pcp096.

A.K. Kushwaha, S. Dwivedi, A. Mukherjee, M. Lingwan, M.A. Dar, L. Bhagavatula, S. Datta, Plant microProteins: small but powerful modulators of plant development, iScience 25 (11) (2022) 105400, https://doi.org/10.1016/j.isci.2022.105400.

B. Langmead, S.L. Salzberg, Fast gapped-read alignment with Bowtie 2, Nat. Methods 9 (4) (2012) 357–359, https://doi.org/10.1038/nmeth.1923.

P.O. Lim, H.J. Kim, H.G. Nam, Leaf senescence, Annu. Rev. Plant Biol. 58 (2007) 115–136, https://doi.org/10.1146/annurev.arplant.57.032905.105316.

K.N. Lohman, S. Gan, M.C. John, R.M. Amasino, Molecular analysis of natural leaf senescence in Arabidopsis thaliana, Physiol. Plant. 92 (2) (1994) 322–328, https://doi.org/10.1111/j.1399-3054.1994.tb05343.x.

M.I. Love, W. Huber, S. Anders, Moderated estimation of fold change and dispersion for RNA-seq data with DESeq2, Genome Biol. 15 (12) (2014), https://doi.org/10.1186/s13059-014-0550-8.

D.E. Martinez, M.L. Borniego, N. Battchikova, E.M. Aro, E. Tyystjarvi, J.J. Guiamet, SASP, a Senescence-associated subtilisin protease, is involved in reproductive development and determination of silique number in Arabidopsis, J. Exp. Bot. 66 (1) (2015) 161–174, https://doi.org/10.1093/jxb/eru409.

D.E. Martinez, M.L. Costa, F.M. Gomez, M.S. Otegui, J.J. Guiamet, Senescence-associated vacuoles' are involved in the degradation of chloroplast proteins in tobacco leaves, Plant J. 56 (2) (2008) 196–206, https://doi.org/10.1111/j.1365-313X.2008.03585.x.

J. Mistry, R.D. Finn, S.R. Eddy, A. Bateman, M. Punta, Challenges in homology search: HMMER3 and convergent evolution of coiled-coil regions, Nucleic Acids Res. 41 (12) (2013) e121, https://doi.org/10.1093/nar/gkt263.

M.A. Omidbakhshfard, E.M. Sokolowska, V. Di Vittori, L. Perez de Souza, A. Kuhalskaya, Y. Brotman, S. Alseekh, A.R. Fernie, A. Skirycz, Multi-omics analysis of early leaf development in Arabidopsis thaliana, Patterns 2 (4) (2021) 100235, https://doi.org/10.1016/j.patter.2021.100235.

M.S. Otegui, Vacuolar degradation of chloroplast components: autophagy and beyond, J. Exp. Bot. 69 (4) (2018) 741–750, https://doi.org/10.1093/jxb/erx234.

M.S. Otegui, Y.S. Noh, D.E. Martinez, M.G. Vila Petroff, L.A. Staehelin, R.M. Amasino, J. J. Guiamet, Senescence-associated vacuoles with intense proteolytic activity develop in leaves of Arabidopsis and soybean, Plant J. 41 (6) (2005) 831–844, https://doi.org/10.1111/j.1365-313X.2005.02346.x.

T. Paysan-Lafosse, M. Blum, S. Chuguransky, T. Grego, B.L. Pinto, G.A. Salazar, M. L. Bileschi, P. Bork, A. Bridge, L. Colwell, J. Gough, D.H. Haft, I. Letunic, A. Marchler-Bauer, H. Mi, D.A. Natale, C.A. Orengo, A.P. Pandurangan, C. Rivoire, C. J.A. Sigrist, I. Sillitoe, N. Thanki, P.D. Thomas, S.C.E. Tosatto, C.H. Wu, A. Bateman, InterPro in 2022, Nucleic Acids Res. 51 (D1) (2023) D418–D427, https://doi.org/10.1093/nar/gkac993.

K.C. Rhee, Determination of Total Nitrogen, Curr. Protoc. Food Anal. Chem. (2001), https://doi.org/10.1002/0471142913.fab0102s00.

I.N. Roberts, C. Caputo, M.V. Criado, C. Funk, Senescence-associated proteases in plants, Physiol. Plant. 145 (1) (2012) 130–139, https://doi.org/10.1111/j.1399-3054.2012.01574.x.

I.N. Roberts, C. Caputo, M. Kade, M.V. Criado, A.J. Barneix, Subtilisin-like serine proteases involved in N remobilization during grain filling in wheat, Acta Physiol. Plant. 33 (5) (2011) 1997–2001, https://doi.org/10.1007/s11738-011-0712-1.

Y. Sakuraba, Light-mediated regulation of leaf Senescence, Int. J. Mol. Sci. 22 (7) (2021), https://doi.org/10.3390/ijms22073291.

A. Schreiber, M. Peter, Substrate recognition in selective autophagy and the ubiquitin-proteasome system, Biochim. Et. Biophys. Acta 1843 (1) (2014) 163–181, https://doi.org/10.1016/j.bbamcr.2013.03.019.

L. Taiz, E. Zeiger, Møller, Murphy A. IM, Plant Physiology and Development, 6, Sinauer Associates Incorporated, 2015 (vol Ed).

E. Tamary, R. Nevo, L. Naveh, S. Levin-Zaidman, V. Kiss, A. Savidor, Y. Levin, Y. Eyal, Z. Reich, Z. Adam, Chlorophyll catabolism precedes changes in chloroplast structure and proteome during leaf senescence, Plant Direct 3 (3) (2019) e00127, https://doi.org/10.1002/pld3.127.

M.A. Taylor, P.D. Fraser, Solanesol: added value from Solanaceous waste, Phytochemistry 72 (11-12) (2011) 1323–1327, https://doi.org/10.1016/j.phytochem.2011.03.015.

G. Tcherkez, A. Carroll, C. Abadie, S. Mainguet, M. Davanture, M. Zivy, Protein synthesis increases with photosynthesis via the stimulation of translation initiation, Plant Sci. 291 (2020) 110352, https://doi.org/10.1016/j.plantsci.2019.110352.

A. Tiessen, P. Pérez-Rodríguez, L.J. Delaye-Arredondo, Mathematical modeling and comparison of protein size distribution in different plant, animal, fungal and microbial species reveals a negative correlation between protein size and protein number, thus providing insight into the evolution of proteomes, BMC Res. Notes 5 (2012) 85, https://doi.org/10.1186/1756-0500-5-85.

L.C. van Loon, H.C.P.M. van der Valk, A.J. Haverkort, G.L. Lokhorst, Changes in protease activity in leaves during natural development and accelerated ageing upon detachment, J. Plant Physiol. 127 (3-4) (1987) 339–353, https://doi.org/10.1016/s0176-1617(87)80152-9.

K.J. Van Wijk, Protein maturation and proteolysis in plant plastids, mitochondria, and peroxisomes, Annu. Rev. Plant Biol. 66 (1) (2015) 75–111, https://doi.org/10.1146/annurev-arplant-043014-115547.

H. Wang, J.H.M. Schippers, The role and regulation of autophagy and the proteasome during aging and senescence in plants, Genes 10 (4) (2019), https://doi.org/10.3390/genes10040267.

Y. Yu, M. Kleuter, S. Taghian Dinani, L.M. Trindade, A.J. van der Goot, The role of plant age and leaf position on protein extraction and phenolic compounds removal from tomato (Solanum lycopersicum) leaves using food-grade solvents, Food Chem. 406 (2023) 135072, https://doi.org/10.1016/j.foodchem.2022.135072.

Y. Yu, M. Kleuter, L.M. Trindade, A.J. van der Goot, Tomato (Solanum lycopersicum) leaf juice as enzyme source: a study on the impact of endogenous proteases on plant proteins, Food Hydrocoll. 155 (2024), https://doi.org/10.1016/j.foodhyd.2024.110245.

L.F. Zhang, Q. Rui, P. Zhang, X.Y. Wang, L.L. Xu, A novel 51-kDa fragment of the large subunit of ribulose-1,5-bisphosphate carboxylase/oxygenase formed in the stroma of chloroplasts in dark-induced senescing wheat leaves, Physiol. Plant. 131 (1) (2007) 64–71, https://doi.org/10.1111/j.1399-3054.2007.00928.x.

A. Zhu, J.G. Ibrahim, M.I. Love, Heavy-tailed prior distributions for sequence count data: removing the noise and preserving large differences, Bioinformatics 35 (12) (2019) 2084–2092, https://doi.org/10.1093/bioinformatics/bty895.

X. Zhuang, L. Jiang, Chloroplast degradation: multiple routes into the vacuole, Front. Plant Sci. 10 (2019) 359, https://doi.org/10.3389/fpls.2019.00359.